Fabrication of novel particle electrode γ-Al_2O_3@ZIF-8 and its application for degradation of Rhodamine B

Liguo Zhang[1*], Caixia Ma[1], Lei Liu[2*], Jingshi Pan[1], Qilin Wang[3]

1. School of Environment, South China Normal University; Guangdong Provincial Engineering Technology Research Center for Wastewater Management and Treatment, Guangzhou 510006, China

2. School of Environment and Civil Engineering, DongGuan University of Technology, DongGuan 523808, China

3. Centre for Technology in Water and Wastewater, School of Civil and Environmental Engineering, University of Technology Sydney, Ultimo, NSW 2007, Australia

[*]Corresponding authors

Liguo Zhang, E-mail: zhanglg@scnu.edu.cn

Tel: +86-20-39310213

Fax: +86-20-39310187

Lei Liu, E-mail: liulei97@126.com

Tel: +86-769-22861232

Abstract

Due to the high Brunauer-Emmet-Teller (BET) surface area of zeolitic imidazolate framework (ZIF)-8, secondary crystallization method was used to prepare particle electrode γ-Al_2O_3@ZIF-8. According to the results from field emission scanning electron microscope (SEM) and X-ray diffractometer (XRD), the particle electrode γ-Al_2O_3 was successfully loaded with ZIF-8, and the BET surface area (1433 m^2/g) of ZIF-8 was over 10 times than that of γ-Al_2O_3. The key operation parameters of cell voltage, pH, initial RhB concentration and electrolyte concentration were all optimized. The observed rate constant (k_{obs}) of pseudo-first-order kinetic model for the electrocatalytic oxidation (ECO) system with particle electrode γ-Al_2O_3@ZIF-8 (15.2×10^{-2} min^{-1}) was over 5 times higher than that of the system with traditional particle electrode γ-Al_2O_3 (2.6×10^{-2} min^{-1}). The loading of ZIF-8 on the surface of γ-Al_2O_3 played an important role in improving electrocatalytic activity for the degradation of Rhodamine B (RhB), and the RhB removal efficiency of the 3D electrocatalytic system with particle electrode of γ-Al_2O_3@ZIF-8 was 93.5% in 15 min, compared with 27.5% in 15 min for particle electrode γ-Al_2O_3. The RhB removal efficiency was kept over 85% after five cycles of reuse for the three-dimensional (3D) electrocatalytic system with particle electrode of γ-Al_2O_3@ZIF-8.

Keywords: particle electrode; electrocatalytic oxidation (ECO); zeolitic imidazolate framework (ZIF)-8; RhB

1. Introduction

Printing and dyeing mill generates a large amount of dye-rich effluents which contain some bio-refractory organic complicated compounds. Even after the biodegradation or chemical flocculation treatment(Holkar *et al.* 2016), there still exists some of these substances, such as Rhodamine B (RhB), methyl orange and malachite green(Yu *et al.* 2018). Considering the aesthetic and toxicity problem, it is indispensable to degrade these pigments completely. So far, attempts have been made to degrade and destroy those pigments using diverse advanced oxidation processes (AOPs), including photochemical or electrochemical reactions, ozonation, Fenton oxidation, and catalytic wet oxidation(He *et al.* 2019). In comparison to other AOPs, electrocatalytic oxidation (ECO) technologies have made great progress in wastewater treatment due to its high efficiency, environmental friendly and versatility(Rana *et al.* 2019).

The present ECO technologies have developed from the two-dimensional (2D) system to the three-dimensional (3D) electrocatalysis oxidation system, which has become a promising technology and is widely employed in wastewater treatment. In 3D electrocatalysis oxidation systems, particle electrodes can be prepared using mesoporous material, such as granular active carbon (GAC), carbon aerogel (CA), metal particles, modified kaolin, and metal oxides(Zhang *et al.* 2010; Hardjono *et al.* 2011; Chu *et al*.,2016; Zhang *et al.* 2013; Moreira *et al.* 2017; Long *et al.* 2019).

Considering the large Brunauer-Emmet-Teller (BET) surface area and electro-adsorption capacity of metal organic frameworks (MOFs), the preparation of particle electrode using MOFs may be an attractive option(Duan *et al.* 2016; Ren *et al.* 2017). However, on account of nanostructure of most MOFs materials, it is difficult to prepare the dimensionally stable particle electrodes using MOFs. Thus, as one of the mesoporous materials, the dimensionally stable γ-alumina (γ-Al_2O_3) can be potentially chosen as the carrier of MOFs. Zeolitic imidazolate frameworks (ZIFs) belong to a special subclass of MOFs. In comparison to other MOFs, ZIFs morphology is

usually stable in aqueous solution and organic solvents, especially ZIF-8(Wang *et al.* 2008). To the best of our knowledge, the application of MOFs in wastewater treatment was reported mainly on adsorptive removal of methyl orange and methylene blue from aqueous solution (Haque *et al.* 2010). The active roles of ZIF-8 on the enhanced visible photocatalytic activity of Ag/AgCl were also examined for RhB removal, which can be attributed to both adsorption and generation of superoxide radical (Liu *et al.* 2017). An iron terephthalate metal-organic framework MIL-53(Fe) synthesized by a facile solvothermal reaction was capable of activating hydrogen peroxide (H_2O_2) to achieve high efficiency in photocatalytic process (Ai *et al.* 2014). However, there are still some shortcomings limiting their industrial application of the ECO technologies, such as short lifetime of electrode materials and low current efficiency due to some intrinsic drawbacks such as mass transfer limitation, small space-time yield, and low area-volume ratio. Therefore, it is important to develop new particle electrode for improving area-volume ratio and current efficiency.

In this study, particle electrode developed from ZIF-8 material was first proposed and the preparation process was optimized. Characterization and performance research of the particle electrode were also carried out. Moreover, this study was committed to supplying a useful base and reference for practical application of 3D electrochemical degradation on dying wastewater treatment. RhB was used as the representative target substance to prepare the simulated wastewater to evaluate the electrochemical performance of prepared particle electrodes. The effects of operating parameters, such as cell voltage, pH, initial RhB concentration and electrolyte concentration, on the RhB degradation were all examined. The mechanisms for RhB removal and the reusability of particle electrode were both investigated.

2. Experimental section

2.1. Materials

Zinc nitrate hexahydrate ($Zn(NO_3)_2 \cdot 6H_2O$), methanol, zinc chloride, sodium formate and sodium sulphate anhydrous were purchased from Guangzhou chemical reagent factory. 2-methylimidazole was purchased from Macklin. All of these reagents were of analytical purity grade. γ-Al_2O_3 (BET surface area: 140 m^2/g, pore volume: 0.386 cm^3/g) with the diameters of 3-5 mm was purchased from Dongzi science and technology co., LTD, China. Titanium electrode (5 cm×5 cm×1 mm) and Ti/RuO_2(5 cm×5 cm×1 mm) electrode were purchased from Zhao bond metal composite material co., LTD, China.

2.2. Preparation of particle electrode γ-Al_2O_3@ZIF-8

In this study, γ-Al_2O_3 was used as the support for the synthesis of particle electrode. The γ-Al_2O_3 particles were washed with tap-water and deionized water for three times under ultrasonication, and then were baked in the muffle furnace at 823 K for 6 h with 1 k/min heating rate.

In a standard synthesis of ZIF-8 crystals (Venna *et al.* 2010), 70mL methanol containing 3.3 g 2-methylimidazole was poured into the equal volume solution containing 1.5 g ($Zn(NO_3)_2 \cdot 6H_2O$). The mixture was stirred for 24 h at room temperature (298±1 K). The product was collected by centrifuging, washed with methanol for three times, and then dried at 353 K overnight in a drying oven for further research.

The powdered sample ZIF-8 was dissolved in methanol in a certain proportion and the well-distributed suspended solution was obtained under ultrasound for 10 minutes. The dry γ-Al_2O_3 was dipped into the above-mentioned suspended solution for 5 min. After that period, the particles were taken out from the solution and dried at room temperature for 3 hours, then dried at 393 K for 24 h. Thus, the particles loading ZIF-8 seed layer were obtained, used as the support for secondary growth of ZIF-8 membranes (Xu *et al.* 2011).

The particles loading ZIF-8 seed layer were tiled at the bottom in a Teflon-lined autoclave, followed by slowly pouring ZIF-8 synthesis solution containing $ZnCl_2$, 2-methylimidazole, sodium formate and methanol into the autoclave, and then sealed and heated in a stainless steel autoclave at 393 K for 4 h, then cooled down to room

111 temperature. The resulting particles were washed with methanol for three times and dried at room temperature for
112 24 h, then γ-Al_2O_3@ZIF-8 was obtained.

113 *2.3. Electrocatalytic setup and operation*

114 The 3D-electrochemical degradation of RhB was carried out in a rectangular undivided organic glass cell of
115 585 mL (13cm×9cm×5cm) capacity. In the system, a Ti/RuO_2 electrode and a Ti electrode were used as the anode
116 and the cathode, respectively. The available working surface of two electrodes was 15cm^2 (5cm×3cm). The anode
117 and cathode were situated vertically and parallel to each other with an inner gap of 4 cm to position a given volume
118 of particle electrodes, which were immersed in the simulated wastewater for 24 h prior to its use. Every particle
119 with high independence would serve as an electrolysis cell in the system, thus the electrodes areas were increased
120 greatly. The particle electrodes were placed in a support netted container in the 3D electrocatalytic system. 450 mL
121 of RhB solution was transferred into the reactor. Na_2SO_4 was added into the RhB solution to enhance the
122 conductivity and adjust the initial solution pH before electro-degradation. A DC power supply (RXN 305D, China)
123 was employed to connect with anode and cathode. The compressed air was sparged into 3D electrode reactor from
124 the bottom at 0.04 m^3/h, the compressed air was used to provide oxygen and accelerate mass transfer of RhB.

125 *2.4. Optimization of influence factors for RhB degradation*

126 The effects of cell voltage, pH, initial RhB concentration and electrolyte concentration on the electrocatalytic
127 degradation of RhB were examined, the design of laboratory batch tests was shown in Table 1. Typically, 450 mL
128 of RhB solution was used for tests and all samples were measured in triplicates. To exclude the effect of adsorptive
129 removal on RhB degradation, the 3D electrocatalytic system was immersed in the simulated wastewater for 24 h
130 each test prior to its use. And the RhB samples were collected at every 5 min after the start of the treatment until
131 complete removal of RhB. (The results are shown in Supplementary Material).

132 *2.5. Comparison of electrocatalytic activity for RhB degradation and kinetics analysis*

Under the obtained optimum operation parameters, the degradation of RhB was comparatively investigated with particle electrode of γ-Al_2O_3 and γ-Al_2O_3@ZIF-8. In order to compare the electrocatalytic activity, the degradation of RhB was fitted using a pseudo-first-order kinetic model, as described by the following equation (Diao *et al.* 2017):

$$\ln(C_t/C_0) = -k_{obs} \cdot t \quad (1)$$

where C_t is the concentration of RhB at selected time (mg/L), C_0 is the initial RhB concentration (mg/L), k_{obs} is the observed rate constant (min^{-1}), and t is time (min).

Table 1 Design of the batch tests for study on influence factors of RhB degradation

Group	Influence factors	Other operation parameters
1. Effect of cell voltage/ V	8 10 15 20 25	Initial pH of 2.0, 20 mg/L RhB, 8 g/L of Na_2SO_4
2. Effect of pH	2.0 4.0 6.0 9.0 11.0	Cell voltage of 20 V, 20 mg/L RhB, 8 g/L of Na_2SO_4
3. Effect of initial RhB concentration/ mg/L	10 20 40 60	Cell voltage of 20 V, initial pH of 2.0, 8 g/L of Na_2SO_4
4. Effect of electrolyte concentration/ g/L	2 4 8 16	Cell voltage of 20 V, initial pH of 2.0, 20 mg/L RhB

2.6. Experiments for mechanisms of RhB degradation

In order to demonstrate the mechanisms of RhB degradation with particle electrode of γ-Al_2O_3@ZIF-8, two identical electrocatalytic systems were comparatively examined. One was used as control without Tertiary butyl

alcohol (TBA) addition, the other was added 1% (v/v) of TBA as a hydroxyl radical (·OH) quencher. The experiment was carried out at the optimum conditions that determined based on the above experiments: cell voltage of 20 V, pH of 2.0, initial RhB concentration of 20 mg/L and electrolyte concentration of 8 g/L. The collection and measurements of samples were same as above-mentioned steps.

2.7. Reuse tests

In order to examine the reusability of novel particle electrode of γ-Al_2O_3@ZIF-8 in a 3D electrocatalytic system for RhB degradation, as the typical steps for preparation of 450 ml of RhB solution and the 3D electrocatalytic system, the optimum operation parameters of cell voltage of 20 V, pH of 2.0, initial RhB concentration of 20 mg/L, 8 g/L of Na_2SO_4 were used and the treatment time was 60 min. The RhB degradation tests were carried out repeatedly for 5 times, the collection and measurements of samples were same as above-mentioned steps. (The results are shown in Supplementary Material).

2.8. Analytical methods

The morphology and energy dispersive spectrometer (EDS) of particle electrode were characterized by field emission scanning electron microscope (SEM, ZEISS Ultra 55, Germany, Carl Zeiss). BET surface area and micropore distribution of ZIF-8 were measured by N_2 adsorption at 77 K on an ASAP2020 equipment. X-ray diffractometer (XRD, Rigaku MiniFlex 600) was employed to analyze the crystal structures of the particle electrodes. Fourier transform infrared (FTIR) spectra of the particle electrodes were investigated with fourier transform infrared spectrometer (FTIR Spectrometer, Nicolet 6700, Thermo Nicolet). Before measurement, the particle electrodes were dehydrated under vacuum at 393 K for 12 h. The RhB concentration was measured with UV-vis spectrometer (UV6000PC, China) at its maximum absorption wavelength of 554 nm. The initial pH of the simulated wastewater was measured with a DZS-706 multi-parameter water quality meter (Rex electric Chemical, Shanghai, China).

3. Results and discussion

3.1. Characterization

The SEM images of the particle electrode are shown in Fig. 1. Apparently, no matter from the top view or the cross-section view, compact hexahedral crystals could be observed on the outer surfaces of the γ-Al_2O_3@ZIF-8. The images also display that the average crystal sizes and the film thickness are about 15 μm and 30 μm, respectively. That indicated a large quantity of ZIF-8 crystals had been growing on the surface of the γ-Al_2O_3 successfully. Fig. 2 shows N_2 adsorption-desorption isotherms (a) and micropore distribution (b) of ZIF-8. On account of the nano-structure and high BET surface area of ZIF-8 (1433 m^2/g) compared with that of γ-Al_2O_3 (140 m^2/g), the adsorption capacity of the γ-Al_2O_3@ZIF-8 was increased, correspondingly, the performance of particle electrode might be improved.

It is well known that as one of MOFs, ZIF-8 has the property of permanent microporosity and tremendous BET specific surface areas. Considering the theory of carbon fiber felt (ACF) used as electrodes in electro-catalysis (Huang & Su 2010), large BET specific surface areas and electrical conductivity could improve the efficiency and reproducibility.

The impregnation process is the key to obtain γ-Al_2O_3@ZIF-8 in our synthesis method. To ensure that the ZIF-8 crystals have been successfully loaded on the γ-Al_2O_3 particle, XRD and IR were employed to analyze the structures and functional groups of the γ-Al_2O_3 and γ-Al_2O_3@ZIF-8. Fig. 3 and Fig. 4 display XRD patterns and IR spectrograms of the particles before and after loading, respectively. Both of the spectrograms of γ-Al_2O_3@ZIF-8 seem to be homologous with γ-Al_2O_3substantially and yet appear some main characteristic peaks of ZIF-8, which were pointed out in the figures. The diffraction peaks of γ-Al_2O_3@ZIF-8 are relatively weak, which results from the relatively lower content of ZIF-8. Another possible reason is weak crystalline during secondary growth.

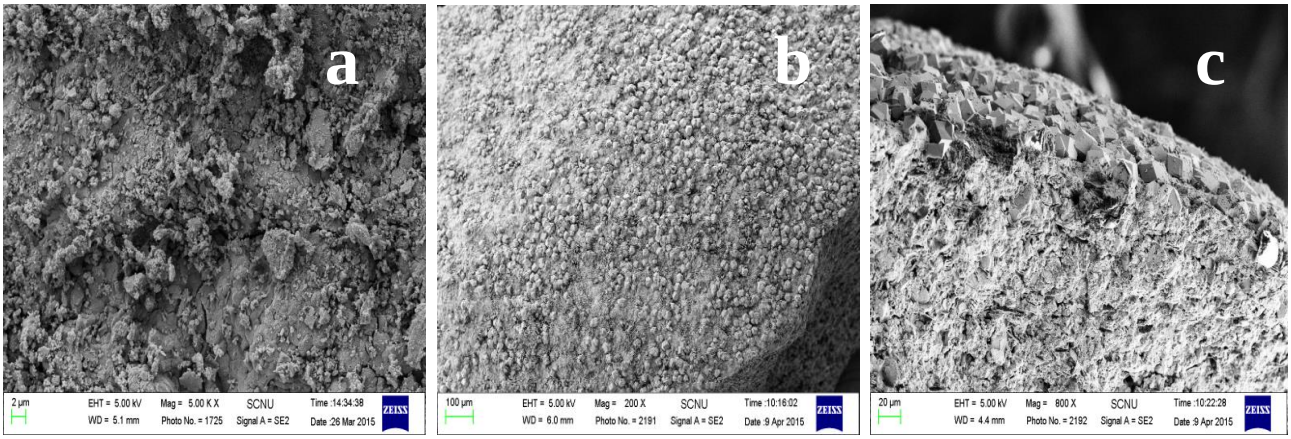

(a) Top view of the γ-Al_2O_3 (b) Top view of the γ-Al_2O_3@ZIF-8 (c) Cross-section of the γ-Al_2O_3@ZIF-8

Fig. 1 SEM images of the particles

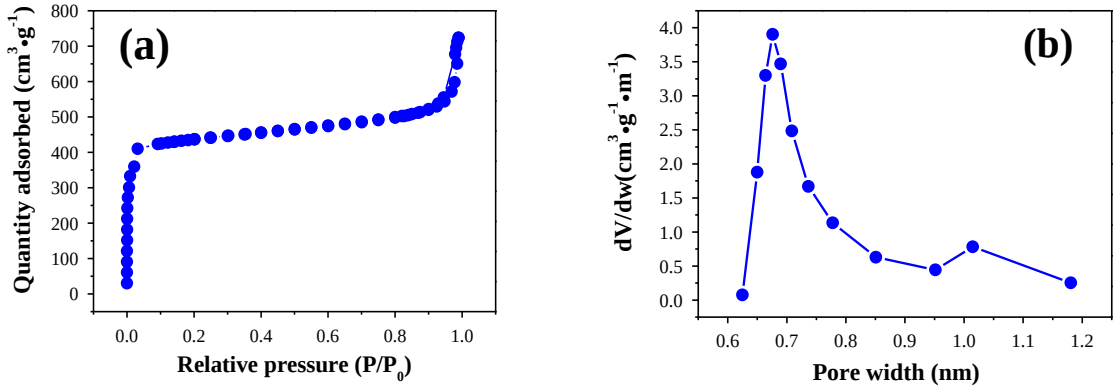

Fig. 2 N_2 adsorption-desorption isotherms (a) and micropore distribution (b) of ZIF-8

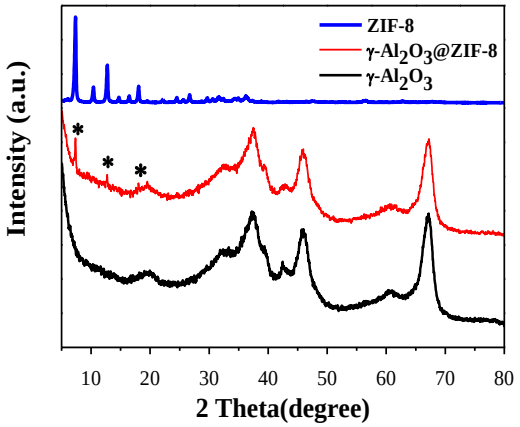

Fig. 3 X-ray diffraction patterns of the particles

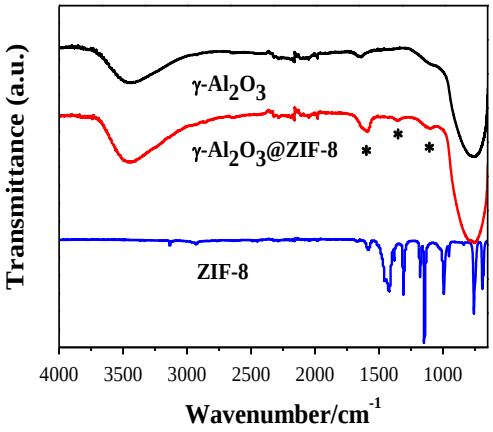

Fig. 4 IR spectra of the particles

197 *3.2. Comparison of RhB degradation with γ-Al_2O_3, γ-Al_2O_3@ZIF-8 and kinetics analysis*

198 The degradation efficiency of RhB with the prepared particle electrode γ-Al_2O_3@ZIF-8 was investigated,
199 compared with traditional particle electrode γ-Al_2O_3. As shown in Fig. 5(a), the particle electrode γ-Al_2O_3@ZIF-8
200 decolorized RhB more effectively than electrode γ-Al_2O_3. The RhB removal rate for the system with particle
201 electrode γ-Al_2O_3@ZIF-8 reached over 93.5% in 15 min. In contrast, the removal rate of RhB for the
202 electrocatalytic system with particle electrode γ-Al_2O_3 only reached 27.5% in 15 min and reached 90% after the
203 treatment for 90 min. Ai et al. employed an iron terephthalate metal-organic framework MIL-53(Fe) to achieve
204 high efficiency in photocatalytic degradation of RhB, with the presence of hydrogen peroxide (H_2O_2), under visible
205 light irradiation within 50 min, and found that the removal efficiency of RhB was less than 85% in 20 min(Ai *et al.*
206 2014). Liu et al. prepared a novel Ag/AgCl/ZIF-8(50%) composite photocatalyst for the removal of RhB from
207 aqueous solution, and found that the removal efficiency of RhB was less than 80% in 30 min with the synthesized
208 Ag/AgCl/ZIF-8(50%). It was also found that both the adsorption ability of ZIF-8 and the ability for the formation
209 of $O_{2^{\cdot}}^{-}$ contributed to the degradation of RhB (Liu *et al.* 2017). Compared with the previous studies, the higher
210 RhB removal efficiency was obtained at shorter reaction time for the 3D electrocatalytic system with particle
211 electrode γ-Al_2O_3@ZIF-8 addition.

212 As shown in Fig. 5(b), the kinetics of electrocatalytic degradation of RhB were pseudo-first order, and the
213 observed rate constant (k_{obs}) of the ECO system with particle electrode γ-Al_2O_3@ZIF-8 (15.2×10^{-2} min^{-1}) was over
214 5 times higher than that of the system with traditional particle electrode γ-Al_2O_3 (2.6×10^{-2} min^{-1}), which suggested
215 that the loading of ZIF-8 on the surface of particle electrode γ-Al_2O_3 enhanced greatly the electrocatalytic activity
216 of 3D ECO system.

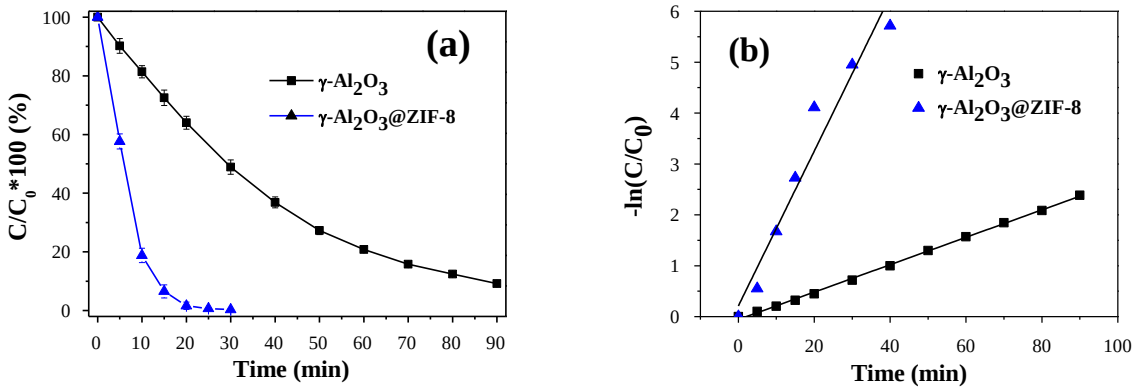

Fig. 5 Time-course variation with different particle electrodes (a) C/C_0 of RhB solution and (b) Pseudo-first order kinetics for the degradation of RhB

3.3. Mechanisms for RhB degradation with particle electrode γ-Al_2O_3@ZIF-8

As shown in Fig. 6, the absorption spectrum of RhB was characterized by its maximum absorbance at 554nm and the absorbance peaks declined obviously with prolonged reaction time due to electrochemical degradation. Natarajan et al. (2011) also reported the study on UV-LED/TiO_2 process for degradation of RhB, and found that the formed intermediate compounds were similar to previously reported literature on the degradation of RhB, the formed oxidized products were mineralized into CO_2, H_2O, NO_3^- and NH_4^+. It was inferred that the degradation of RhB by the photogenerated active species such as •OH and hole could attack the central carbon of RhB to decolorize the dye and further degraded via N-de-ethylation process. The adsorptive removal of RhB was excluded through immersing particle electrode for 24h prior to its use. However, the direct quantitative comparison of RhB removal between electrocatalytic oxidation and the available technologies are difficult since lots of factors (e.g. initial RhB concentration, operating conditions, among others) could affect the results. The higher RhB removal efficiency of 3D electrocatalytic system with particle electrode of γ-Al_2O_3@ZIF-8 is favorable for increasing treatment capacity for dying wastewater.

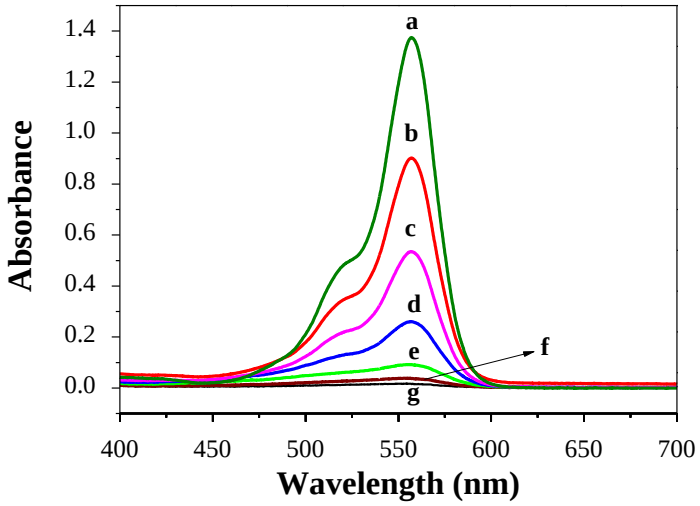

Fig. 6 UV–vis spectra of RhB with γ-Al_2O_3@ZIF-8 electrodes at various treating time: (a) 0 min; (b) 5 min; (c) 10 min; (d) 15 min; (e) 20 min; (f) 25 min; (g) 30 min. Cell voltage of 20 V, pH of 2.0, initial RhB concentration of 20 mg/L, Na_2SO_4 of 8 g/L as supporting electrolyte.

The TBA is a commonly used ·OH radical scavenger and reacts with hydroxyl radicals with a rate constant of 6×10^8 $M^{-1}\cdot s^{-1}$ (Ikhlaq et al., 2012). As shown in Fig. 7, the experimental results showed that the RhB degradation efficiency for the system with the addition of TBA was obviously lower than that with no TBA addition, which also suggested that hydroxyl radical played an important role in the electrocatalytic degradation of RhB. It could be attributed to the disintegration of the azo linkage (conjugated xanthene ring), which acted as the chromophore of RhB (Yan *et al.* 2011). This is probably because ·OH radicals attacked the N=N bond of the azo dye, which maybe the most active site. According to the SEM (Fig. 1) and XRD (Fig. 3) results, ZIF-8 was successfully supported on the outer surface of γ-Al_2O_3.

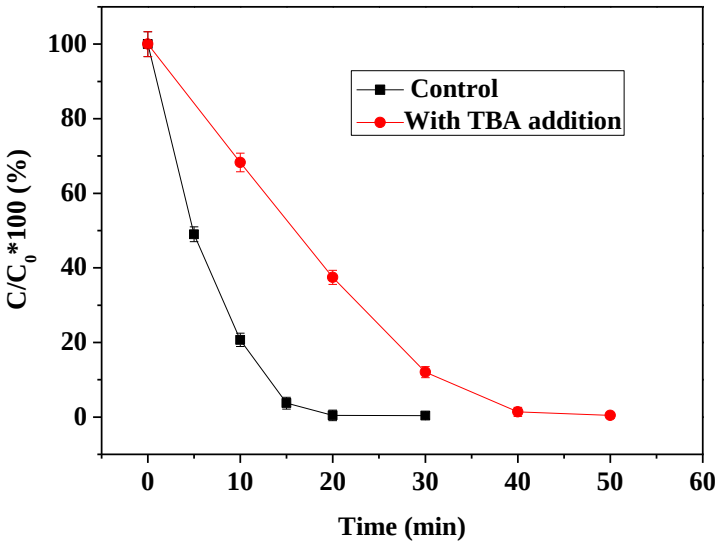

Fig. 7 Effect of 1% (v/v) TBA addition on RhB removal

Fig. 8 shows the mechanisms of hydroxyl radical generation in 3D electrocatalytic system with particle electrode γ-Al_2O_3@ZIF-8. There were two pathways to generate hydroxyl radical: on the anode and particle electrode. At an appropriate voltage, the particles were polarized to form lots of charged microelectrodes with one surface as anode while the other was charged the opposite. The generation of hydroxyl radical on the surface of particle electrode can be expressed as Formula 4 and Formula 5 (Zhang *et al.* 2013). On the other hand, the BET surface area of ZIF-8 was 1433 m^2/g and was much higher than that of the carrier γ-Al_2O_3, which could enhance greatly the adsorption capacity for RhB and accelerate the mass transfer rate of RhB on liquid-solid interface, resulting in high efficiency of RhB degradation.

$$O_2 + 2H^+ + 2e^- \rightarrow H_2O_2 \quad (4)$$

$$H_2O_2 \rightarrow 2 \cdot OH \quad (5)$$

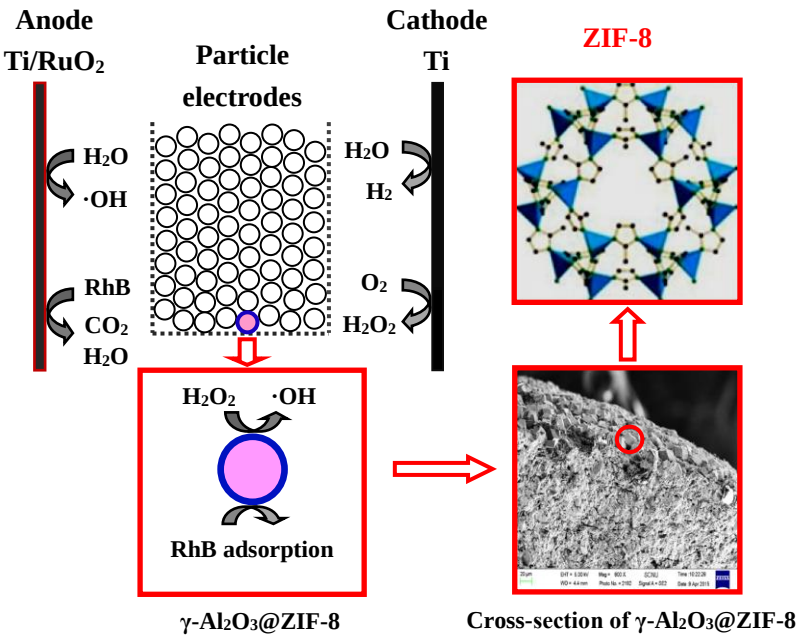

Fig. 8 Mechanisms of hydroxyl radical generation in 3D electrocatalytic system with particle electrode γ-Al_2O_3@ZIF-8

4. Conclusions

In summary, we demonstrated that the novel particle electrode of γ-Al_2O_3@ZIF-8 showed good electrocatalytic activity and reusability for RhB degradation in a 3D electrochemical system. The electrocatalytic activities depended greatly on the various operating parameters. The results on hydroxyl radical quencher by TBA showed that the loading of ZIF-8 on the surface of γ-Al_2O_3 played an important role in improving electrocatalytic activity for RhB degradation, and the RhB removal efficiency of the electrocatalytic system with particle electrode of γ-Al_2O_3@ZIF-8 was 93.5% in 15 min. The high RhB removal efficiency and reusability of particle electrode γ-Al_2O_3@ZIF-8 in the ECO system make it become a promising treatment technology for dye wastewater.

Acknowledgements

This research was financially supported by the Nature Science Foundation of Guangdong Province (No.

2016A030313432) and the Outstanding Young Innovative Talent Training Plan of Guangdong Universities (No. 2012LYM_0050). Dr. Qilin Wang acknowledges the support of Australian Research Council Discovery Early Career Researcher Award (DE160100667).

References

Ai L., Zhang C., Li L. & Jiang J. 2014 Iron terephthalate metal-organic framework: Revealing the effective activation of hydrogen peroxide for the degradation of organic dye under visible light irradiation. *Applied Catalysis B: Environmental*, **148-149**, 191-200.

Chu H.Q., Wang Z., Liu Y., 2016 Application of modified bentonite granulated electrodes for advanced treatment of pulp and paper mill wastewater in three-dimensional electrode system. *J. Envir. Chem.Eng.*,**4**,1810-1817.

Diao Z.H., Liu J.J., Hu Y.X., Kong L.J., Jiang D. & Xu X.R. 2017 Comparative study of Rhodamine B degradation by the systems pyrite/H_2O_2 and pyrite/persulfate: Reactivity, stability, products and mechanism. *Sep. Purif. Technol.*, **184**, 374-383.

Duan X., Wang H. Z., Ji Z. G., Cui Y. J., Yang Y. and Qian G. D. 2016 A novel metal-organic framework for high storage and separation of acetylene at room temperature. *Journal Of Solid State Chemistry* **241**, 152-6.

Haque E., Lee J.E., Jang I.T., Hwang Y.K., Chang J.S., Jegal J. & Jhung S.H. 2010 Adsorptive removal of methyl orange from aqueous solution with metal organic frameworks, porous chromium-benzenedicarboxylates. *J. Hazard. Mater.*, **181**, 535-542.

Hardjono Y., Sun H., Tian H., Buckley C.E. & Wang S. 2011 Synthesis of Co-oxide doped carbon aerogel catalyst and catalytic performance in heterogeneous oxidation of phenol in water. *Chem. Eng. J.*, **174**, 376-382.

He Y. P., Lin H. B., Guo Z. C., Zhang W. L., Li H. D. and Huang W. M. 2019 Recent developments and advances in boron-doped diamond electrodes for electrochemical oxidation of organic pollutants. *Separation and*

298 *Purification Technology* **212**, 802-21.

299 Holkar C. R., Jadhav A. J., Pinjari D. V., Mahamuni N. M. and Pandit A. B. 2016 A critical review on textile

300 wastewater treatments: Possible approaches. *Journal Of Environmental Management* **182**, 351-66.

301 Huang C.C. & Su Y.J. 2010 Removal of copper ions from wastewater by adsorption/electrosorption on modified

302 activated carbon cloths. *J. Hazard. Mater.*, **175**, 477-483.

303 Ikhlaq A., Brown D.R., Kasprzyk-Hordern B., 2012 Mechanisms of catalytic ozonation on alumina and zeolites in

304 water: Formation of hydroxyl radicals. Applied Catalysis B: Environmental 123-124: 94-106.

305 Liu J., Li R., Wang Y., Wang Y., Zhang X. & Fan C. 2017 The active roles of ZIF-8 on the enhanced visible

306 photocatalytic activity of Ag/AgCl: Generation of superoxide radical and adsorption. *Journal of Alloys and*

307 *Compounds*, **693**, 543-549.

308 Long Y. Y., Feng Y., Li X., Suo N., Chen H., Wang Z. W. and Yu Y. Z. 2019 Removal of diclofenac by

309 three-dimensional electro-Fenton-persulfate (3D electro-Fenton-PS). *Chemosphere* **219**, 1024-31.

310 Moreira F. C., Boaventura R. A. R., Brillas E. and Vilar V. J. P. 2017 Electrochemical advanced oxidation

311 processes: A review on their application to synthetic and real wastewaters. *Applied Catalysis*

312 *B-Environmental* **202**, 217-61.

313 Natarajan T.S., Thomas M., Naratajan K., Bajaj H.C. & Tayade R.J. 2011 Study on UV-LED/TiO_2 process for

314 degradation of Rhodamine B dye. *Chem. Eng. J.*, **169**, 126-134.

315 Navalon S., Dhakshinamoorthy A., Alvaro M. & Garcia H. 2011 Heterogeneous fenton catalysts based on activated

316 carbon and related materials. *Chem Sus Chem.*, **4**, 1712-1730.

317 Rana A., Baig N. and Saleh T. A. 2019 lectrochemically pretreated carbon electrodes and their electroanalytical

318 applications - A review. *Journal Of Electroanalytical Chemistry* **833**, 313-32.

319 Ren J. W., Musyoka N. M., Langmi H. W., Mathe M. and Liao S. J. 2017 urrent research trends and perspectives on

materials-based hydrogen storage solutions: A critical review. *International Journal Of Hydrogen Energy* **42**(1), 289-311.

Venna S.R., Jasinski J.B. & Carreon M.A. 2010 Structural evolution of zeolitic imidazolate framework-8. *J. Am. Chem. Soc.*, **132**(51), 18030-18033.

Wang B., Cote A.P., Furukawa H., O'Keeffe M. & Yaghi O.M. 2008 Colossal cages in zeolitic imidazolate frameworks as selective carbon dioxide reservoirs. *Nature*, **453**(7192), 207-211.

Xu G., Yao J., Wang K., He L., Webley P.A., Chen C. & Wang H. 2011 Preparation of ZIF-8 membranes supported on ceramic hollow fibers from a concentrated synthesis gel. *J. Membrane Sci.*, **385-386**, 187-193.

Yan L., Ma H., Wang B., Wang Y. & Chen Y. 2011 Electrochemical treatment of petroleum refinery wastewater with three-dimensional multi-phase electrode. *Desalination*, **276**, 397-402.

Yu Z.J., Rajesh Kumar M., Chu Y., Hao H.X., Wu Q.Y. & Xie H.D. 2018 Photocatalytic decomposition of RhB by newly designed and highly effective CF@ZnO/CdS hierarchical heterostructures. *ACS Sustainable Chem. Eng.*, **6**(1), 155-164.

Zhang C., Jiang Y., Li Y., Hu Z., Zhou L. & Zhou M. 2013 Three-dimensional electrochemical process for wastewater treatment: A general review. *Chem. Eng. J.*, **228**, 455-467.

Zhang H., Li Y. L., Wu X. G., Zhang Y. J. and Zhang D. B. 2010 Application of response surface methodology to the treatment landfill leachate in a three-dimensional electrochemical reactor. *Waste Management* **30**(11), 2096-102.